SEMI-ANNUAL STATUS REPORT

SR-2

Covering Period: August 1, 1970 through January 31, 1971

A STUDY OF THE LOCAL PRESSURE FIELD IN TURBULENT SHEAR FLOW AND ITS RELATION TO AERODYNAMIC NOISE GENERATION

Research Grant No. NASA NGR 14-005-149

Nuclear Engineering Program
University of Illinois
Urbana, Illinois 61801

Prepared by : Barclay G. Jones, Associate Professor
Bruce W. Spencer, Research Assistant Professor

Submitted by: *Barclay G. Jones*
Barclay G. Jones
Principal Investigator

Approved by: *Marvin E. Wyman*
Marvin E. Wyman, Chairman
Nuclear Engineering Program

January 31, 1971

TABLE OF CONTENTS

1. SCOPE AND OBJECTIVES

Noise generation by turbulent aerodynamic shear flow is being studied by examination of the fluctuating static pressure field comprised of a pseudosound pressure field, responsible for generating sound, and a true acoustic pressure field. Understanding the interrelation between these pressure fields and the coupled velocity field is fundamental in understanding and subsequently controlling noise emission from jets and other high intensity turbulent shear flows.

The study includes three major aspects:

1) A thorough experimental investigation of both the pseudosound pressure and velocity fields in a well controlled incompressible shear flow is being conducted to provide their detailed statistical structure. Using incompressible flow insures the dominance of the pseudosound over the acoustic sound in the flow field. It also establishes the characteristics of the pseudosound pressure field which is believed to be fundamentally the same in both compressible and incompressible flows. The study will also provide both the Eulerian and the Lagrangian structure of the pseudosound pressure as well as the velocity fields.
2) A detailed analytical examination of Ribner's dilatation formulation [1]* for aerodynamic noise in terms of the experimentally determined characteristics of the pseudosound pressure field is being made. Since the pressure field is a scalar and its characteristics define completely the acoustic source, a model of the mechanics of noise generation is being sought which should be capable of predicting the level, the directional dependence, and the spectrum of the radiated sound.
3) An assessment of the capability of the bleed pressure transducer for making pseudosound pressure measurements in a subsonic compressible jet-flow facility, in which the pseudosound and the acoustic sound fields are both present, is being carried out.

*Numbers in brackets refer to entries in REFERENCES.

2. CURRENT STATUS

Research performed in our laboratory under this contract, prior to the period of this report, resulted in completion of the first two specific objectives of the pseudosound pressure study described in Section 3.4 of the research grant proposal [2]. This work related to the Eulerian frame velocity and pressure characteristics in the plane, two-stream mixing layer, and the results have been reported in Refs. 3 and 4. Work during the preceding six-month contract period has resulted in advancement in several areas of the experimental program and in our data analysis and analytical capabilities.

The expertise and facilities for space-time correlation studies have become a reality in our laboratory. Our new traversing mechanism for axial direction correlations following any turbulence streamline has proved immensely successful. This, and other probing devices, have given us the capability of making two-point correlation measurements with separations in each of the orthogonal coordinate directions. The three sets of correlations obtained are sufficient to establish the vector correlation function defined for pressure by Eqn. 15 in the research proposal [2]. Evaluation of the correlations from recorded two-point turbulence signals has been made possible by the acquisition of a digital correlator and probability analyzer marketed by Thermo-Systems, Inc. Considerable effort has been spent examining the features of this new instrumentation for rapid and accurate turbulence analysis.

Using these techniques and equipment we have initiated the two-part Lagrangian frame turbulence studies. The two parts, as described in Section 3.4 of the research proposal, are comprised of the velocity and pseudosound correlation measurements. At the present time we have completed the velocity measurements and are nearing completion of the velocity data analysis. We recently received the second miniature pressure transducer from TSI, and we are presently preparing for the pressure experiments. These will utilize much the same efforts as were required for the velocity studies. Results from the velocity measurements are presented in Section 3.2.

Planning and design are continuing for the high speed, subsonic jet in which we will be measuring pseudosound pressure and the accompanying noise field. Equipment for this phase of the investigation is being procured. We have obtained a horn driver and a power amplifier for generating a well controlled sound field. This will be used to check measurement systems and to calibrate the miniature pressure transducers. We have placed an order with General Radio Co. for a 1/4-inch B&K condenser microphone and preamplifier system which are compatible with a GR sound and vibration analyzer available in our laboratory.

In October, our research group cooperated in sponsoring a guest lecture on our campus by Dr. J.A.B. Wills of the Aerodynamic Division, National Physical Laboratory, England. Dr. Wills, who at the time was a visiting professor of Aerospace Engineering at Pennsylvania State Univ., has had considerable experience dealing with correlation measurements and analysis in turbulent shear flow. The discussions and information exchanged were of mutual interest and have benefited our research program.

3. WORK ACCOMPLISHED DURING PERIOD OF REPORT

The progress and results of the research program during the period Aug. 1, 1970 - Jan. 31, 1971 will be reviewed briefly in this Section. The work falls into two main categories: experimental and analytical. The former is further divided into Eulerian and Lagrangian subheadings which are described in Sections 3.1 and 3.2, and the latter is described in Section 3.3.

The experimental work pertains to the mixing layer flow regime as described in detail in Refs. 3 and 4. Figure 1 illustrates the mixing layer and defines the velocity ratio, r, which was about 0.3 for the results reported; the primary stream velocity, U_a, was maintained constant at 100 fps. Most measurements have been made in the fully-developed region of the mixing layer at an axial location 22 inches from the point of separation. For reference, Fig. 2 shows the mean velocity, axial component turbulence intensity, and intermittancy profiles at that location.

3.1 Eulerian Properties of the Mean Static Pressure Field

Questions raised in previous work [3,4] about the similarity development of the fluctuating pressure field led to our investigating the development of the mean static pressure field. Measurements of this type are difficult because of the small pressure differences involved and because of the often unreliable response of pressure probes in turbulent shear flow. Several probes were examined, and a small wedge probe was selected because of its excellent spatial resolution, its negligible response to yaw in a direction normal to the shear layer, and its very small response to lateral direction yaw. The pressure was read to 0.0005 inches of water using an inclined manometer.

The results shown in Fig. 3 are for profiles taken at several axial locations. As one can see, the peak magnitudes of the pressure decrement continually increase in the downstream direction. This apparent failure to attain similar profiles may explain the slow development of the fluctuating pressure. It also appears that the mixing layer supports a small pressure difference of about 0.005 $(\Delta h_v)_{a-b}$ between the primary and secondary streams. This is too small a difference to cause noticeable curvature of the mixing layer, but it does result in a higher pressure gradient on the high velocity side. This may further explain the shift of peak p' intensities toward that side of the mixing layer.

3.2 Lagrangian Frame Turbulence Measurements

Two-point correlation measurements were made at x = 22 inches in the fully-developed mixing layer. Wygnanski and Fiedler [5] have shown that correlation functions obtained under similar conditions take on similar profiles in the fully-developed turbulence region. This simplifies the experiment by permitting measurements to be made at only one axial location. The appropriate scaling factor for similarity is simply the distance from the virtual origin, $x - x_0$. All the correlations have therefore been presented in this normalized coordinate frame.

The correlations measured have been for the axial-component velocity fluctuations, u, which define the important spatial scales and Lagrangian frame statistics. The three sets of measurements presented involve separations in the orthogonal directions x, y, z.

The correlation coefficients are defined by

$$R_{11}(\Delta x_i) = \frac{\overline{u(x_i - \frac{\Delta x_i}{2})\, u(x_i + \frac{\Delta x_i}{2})}}{u'(x_i - \frac{\Delta x_i}{2})\, u'(x_i + \frac{\Delta x_i}{2})}$$

where primes denote RMS values. Note that the space separations Δx_i are defined spanning the location x_i. This is experimentally more difficult than a definition based on $u(x_i)\, u(x_i + \Delta x_i)$ since both probes must be moved for each measurement. However, it has the advantage that there is no ambiguity about the location of the measured correlation; it is at x_i rather than at some distance downstream. The notation for the correlation coefficients will be simplified to $R_{\Delta x}$, $R_{\Delta y}$, and $R_{\Delta z}$.

The locations and conditions for the measurements are shown in Fig. 4. The $R_{\Delta x}$ and $R_{\Delta z}$ correlations were obtained at five locations across the mixing layer corresponding to the turbulence centerline, 0.4 intermittancy, and trace intermittancy conditions. The $R_{\Delta y}$ correlation was obtained for separation about the mixing-layer centerline defined by $\phi = 0.5$. The results are shown on Figs. 5-7. In Figs. 5 and 7 it can be seen that the correlations at an intermittancy of 0.4 are almost the same as those measured on the centerline. Hence there is only weak dependence of $R_{\Delta x_i}$ on lateral position in this region, and the results there are well represented by the centerline measurements. Outside this region, however, we are dealing with less and less turbulent fluid and the nature of the correlation changes abruptly. We observe the increasing presence of a discrete frequency, or wavelength, belonging to the irrotational fluctuations of the acoustic near field. These irrotational fluctuations, as we have already found, are impressed by a dominant spectral component of the mixing layer turbulence [5,4]. Another feature to note is that the distributions obtained at corresponding locations on opposite sides of the mixing layer closely match. Since the local velocities at these positions differ greatly, one can see that the local fluctuations are not appreciably the result of local flow conditions. We have also seen [3,4] that the spectral peaks of the irrotational fluctuations on each side of the mixing layer match almost exactly. The only way that both the spatial and frequency characteristics can coincide is for the convection velocity of the wave patterns (rather than the local flow velocity) to be the same. Its magnitude is the flow velocity near the center of the mixing layer which is the region of dominant turbulent motion. Hence it is important in viewing the overall turbulence structure, and subsequently in modeling it, to examine the turbulence characteristics in the region of highest mean shear which, in this case, is at the mixing-layer centerline.

Figure 6 shows that $R_{\Delta y}$ falls to zero at a vertical location corresponding to an intermittancy of .5. An interesting occurrence at larger separations is that the fluctuations become strongly negatively correlated. This follows from what has already been discussed and reflects the similar cause-effect relation between the energy-containing turbulent eddies and the irrotational fluctuations (the acoustic near field) on both sides of the mixing layer. The space-time correlations for this set of measurements are presently being obtained. From preliminary viewing it appears that these will permit evaluation of the velocity at which the waves are transmitted normal to the flow.

Space scales characterizing the dimensions of the energy containing eddies have been obtained from the two-point correlation data. The scales are defined by the equation

$$L_{x_i} = \int_0^{+} R_{\Delta x_i}\, d(\Delta x_i)$$

where the + symbol denotes integration to the first crossing of the zero axis. This eliminates the physically objectional feature of integrating to infinity which is that regions of negative correlation at large separations would lessen the length scales.

The results for the correlation measurements in the turbulence region are summarized in Table 1.

Table 1 Integral Length Scales; r = 0.33, x = 22 inches, U_a = 100 fps.

r	$L_x/(x-x_o)$	$L_y/(x-x_o)$	$L_z/(x-x_o)$	L_x/b	L_y/b	L_x/L_y	L_x/L_z
.4(vs)	.043		.011				
℄	.033	.017	.010	.35	.18	1.97	3.30
.4(hvs)	.035		.011				

The width of the mixing layer, b, is defined as the vertical distance between the rays ϕ = 0.95 and ϕ = 0.05. For the conditions of this experiment, $b/(x-x_o)$ = .094. The integral scales given in Table 1 may be scaled for applicability to mixing layer flow of any velocity ratio (including the step expansion case) by expressing the width in terms of the velocity ratio. Assuming the mean velocity distributions can be fit by Gortler's error function profile:

$$\frac{U - U_b}{U_a - U_b} = \frac{1}{2}\left[1 + \mathrm{erf}(\xi - \xi_o)\right] \tag{1}$$

where $\xi = \sigma y/(x-x_o)$,

and that the spread parameter is given by

$$\frac{\sigma}{\sigma_o} = \frac{1+r}{1-r} = \frac{1}{\lambda} \tag{2}$$

where $\sigma_o = 11$ is the spread parameter for r = o, the width of the mixing layer between $\phi = .95$ and $\phi = .05$ is given by

$$b = \frac{2.34}{\sigma_o}\lambda(x-x_o)$$

$$\therefore \quad b/(x-x_o) = 0.213\,\lambda \qquad \text{for } \sigma_o = 11 \tag{3}$$

Therefore for two fully-developed mixing layer flows the ratio of the thicknesses (or growth rates) is given by

$$\frac{b_1}{b_2} = \frac{\lambda_1}{\lambda_2}, \tag{4}$$

and length scales for arbitrary velocity ratios different from the measurement conditions may be estimated from

$$\frac{L}{(x-x_o)} = \left.\frac{L}{(x-x_o)}\right|_{meas} \frac{\lambda}{\lambda_{meas}} \tag{5}$$

Note that the length scales and mixing layer growth depend only on the velocity ratio and not on the velocity magnitude.

Table 2 presents integral scale data obtained by several investigators for mixing layer flow. The spread of values is surprisingly large and probably reflects different methods of traversing, different methods of data evaluation, and different methods for normalizing the correlation coefficients. (For example, traversing along the x-direction rather than following the local turbulence streamlines, keeping the location of one probe fixed rather than fixing the median location, integration to infinity rather than to the first zero crossing, and normalization by the variance measured by the upstream probe rather than the standard deviations measured by each probe; we have chosen the latter in all instances as being physically more meaningful.) Different experimental apparatus can also have an effect as, for example, in Ref. 5 where an initial trip caused the spread, and therefore the scales, to be larger than generally accepted ($\sigma_o = 9$).

Table 2 Mixing Layer Integral Scales at ∿ Centerline Locations.

Ref	r	L_x/x	L_y/x	L_z/x	L_x/L_y	L_x/L_z
[5]	0	.103	.056	-	1.84	-
[6]	0	.045	(+) (-) .033/.024	.0065	1.36/1.87	6.93
[7]	0	.112	.036	-	3.11	-
[8]	0	.028	-	-	-	-
Present*	0.3	.066	.033	.0193	1.97	3.30

The results of the space-time correlation measurements are shown in Fig. 8. The measurements involve the correlation of signals from two points separated along the ray $\phi = 0.5$ (see Fig. 4); the median location was held constant at $\bar{x} = 22$ inches. The definition of the cross-correlation coefficient written for the axial component velocity fluctuation is

$$R_{\Delta x,\tau} = \frac{\overline{u(\bar{x}+\frac{\Delta x}{2},t)\,u(\bar{x}-\frac{\Delta x}{2},t+\tau)}}{u'(\bar{x}+\frac{\Delta x}{2})\,u'(\bar{x}-\frac{\Delta x}{2})}$$

* Adjusted to r = 0 using Eqn. 5

where τ is the delay time for the upstream probe signals. For every value of spatial separation Δx there is a correlation curve whose optimum delay time corresponds to the point of contact with the envelope [9]. This envelope represents the autocorrelation of the energy-containing motion in the Lagrangian reference frame and the area beneath it is a characteristic integral time scale in the Lagrangian frame.

Comparison of the envelope in Fig. 8 with, for example, the correlation curve for $\Delta x \approx 0$, shows that an eddy maintains its identity while traveling many characteristic length scales. Indeed the eddy structure seems to be very cohesive as evidenced by the fact that the peak correlation has diminished to only 0.2 for a separation $\Delta x/(x-x_0) = .4$ (corresponding to $\Delta x = 9$ inches). The Lagrangian integral time scale has been evaluated from the formula

$$\mathcal{J}_L = \int_0^{\tau_{.2}} R_L(\tau)\, d\tau$$

where $R_L(\tau)$ represents the correlation envelope and $\tau_{.2}$ represents the delay time at which R_L crosses the 0.2 axis. This chopping procedure is made necessary by the failure of R_L to go to zero. In the future this problem may be alleviated by fitting an exponential function to the envelope data. The time scale was determined to be 5.4 msec, and the corresponding Lagrangian frame length scale (determined from the local mean velocity) is 4.2". Hence

$$L_L/(x-x_0) \simeq 0.18\,.$$

Future data analysis on these measurements will include the Fourier Transform of R_L, interpreted as the spectrum function in the moving frame, and the first and higher order derivatives of R_L which are related to the rate of change of the eddy patterns. It is the 4th derivative of the corresponding function defined for the pseudosound pressure field that comprises the acoustic source in the fluctuating fluid flow [2].

3.3 Analytical Lagrangian Frame Turbulent Structure

An analytical study of dispersion in turbulent flows has provided insight into three dimensional turbulence structure in the Lagrangian reference frame [10]. Applying this to the behavior of small, near neutrally bouyant particles suspended in the flow provides a detailed interrelation between the particle and fluid Lagrangian frame statistical behavior. Making the particles neutrally bouyant effectively provides a direct measure of the Lagrangian fluid turbulence. The associated experimental study traces the three-dimensional trajectory of these particles from which the detailed statistical structure of the Lagrangian fluid field is evaluated [11]. The three-dimensional structure of the associated Eulerian fluid turbulence field is obtained by standard hot-film anemometry techniques. Comparison of these results provides insight into this very fundamental turbulence problem. In addition the results will be used for comparison with the space-time correlation approach to Lagrangian statistics being pursued in the jet mixing flow.

Of particular interest is the three dimensional structure since it is highly desirable to develop appropriate models for the convective turbulence of the jet mixing flow field. Examination of the integral parameters, such as time and space scales, relating the two reference frames will be pursued in an attempt to develop appropriate modeling criteria for velocity and pressure fields in mixing flow. Such techniques proved very successful in the dispersion studies mentioned above.

4. FUTURE RESEARCH

Our immediate research plans are two-fold: 1) to continue data analysis for velocity correlation studies, and 2) to initiate and carry out the experimental pseudosound correlations in the fully-developed mixing layer. The pseudosound correlation studies are a principal element of the present investigation and therefore will receive major attention. The experience gained from the experimentally simpler velocity correlations will expedite this effort appreciably. As was necessary in the previous case, the first step will be to examine the disturbance introduced by the upstream probe. This was negligible for the velocity measurements, but, due to the larger probe size, slightly larger offset distances may be required for the pressure measurements. The two-channel data will be FM tape recorded to provide a permanent record of the experiments. The correlations will be obtained for separations in the three coordinate directions at several lateral locations in the mixing layer. This will provide data to evaluate the vector correlation function with which the acoustic source strength for the turbulent flow field may be calculated.

It is also envisioned that design of the high-speed, subsonic jet facility will be finalized and construction carried out during this period. The area surrounding the jet will be acoustically insulated, and every effort will be made to minimize upstream flow noise in the apparatus itself. We anticipate making preliminary pressure fluctuation measurements in the high speed mixing region at the earliest possible time to assess the performances of both the flow facility and the miniature pressure transducers.

The efforts of a graduate assistant, Mr. Peter Planchon, up to this time has centered upon assistance with the experiments and data analysis. In the coming months his efforts will be directed toward the application and extension of Ribner's dilatation formulation for the acoustic source strength in fluctuating flow. He will also become involved in modeling of the turbulence characteristics for analytical prediction of the resulting sound field. These efforts are in preparation for continued study in this area as his Ph.D. thesis research.

5. REFERENCES

1. H. S. Ribner, "The Generation of Sound by Turbulent Jets," in Advances in Applied Mech. 8, pp. 103-187, Ed: H. L. Dryden, Th. Von Karman, G. Kuerti, Academic Press, New York, N. Y. (1964).

2. B. G. Jones, B. W. Spencer, "A Study of the Local Pressure Field in Turbulent Shear Flow and Its Relation to Aerodynamic Noise Generation," Research Proposal to NASA, Nuclear Engineering Program, University of Illinois (1969).

3. B. W. Spencer, "Statistical Investigation of Turbulent Velocity and Pressure Fields in a Two-Stream Mixing Layer," Ph.D. Thesis Dissertation, Nuclear Engineering Program, University of Illinois (1970).

4. B. G. Jones, B. W. Spencer, Semi-annual Status Report, SR-1, for Research Grant No. NASA NGR 14-005-149, July 31, 1970.

5. I. Wygnanski, H. E. Fiedler, "The Two-Dimensional Mixing Region," Jour. Fluid Mech. 41, pp. 327-361 (1970).

6. Bradshaw, P., Ferriss, D. H., and Johnson, R. F., "Turbulence in the Noise-Producing Region of a Circular Jet," Jour. Fluid Mech., 19, 591-624 (1964).

7. J. C. Lawrence, "Intensity, Scale, and Spectra of Turbulence in the Mixing Region of a Free Subsonic Jet," NACA TR 1292 (1956).

8. H. W. Liepman and J. Laufer, "Investigations of Free Turbulent Mixing," NACA TN 1257 (1947).

9. J. A. B. Wills, "On Convection Velocities in Turbulent Shear Flows," J. Fluid Mech. 20, pp. 417-432 (1964).

10. C. C. Meek and B. G. Jones, "On the Transport of Dilute Particulate Suspensions in Turbulent Fluid Fields," submitted for publication.

11. B. G. Jones, B. T. Chao and M. A. Shirazi, "An Experimental Study of the Motion of Small Particles in a Turbulent Fluid Field Using Digital Techniques for Statistical Data Processing," Developments in Mechanics, 4, 1249-1274 (1968).

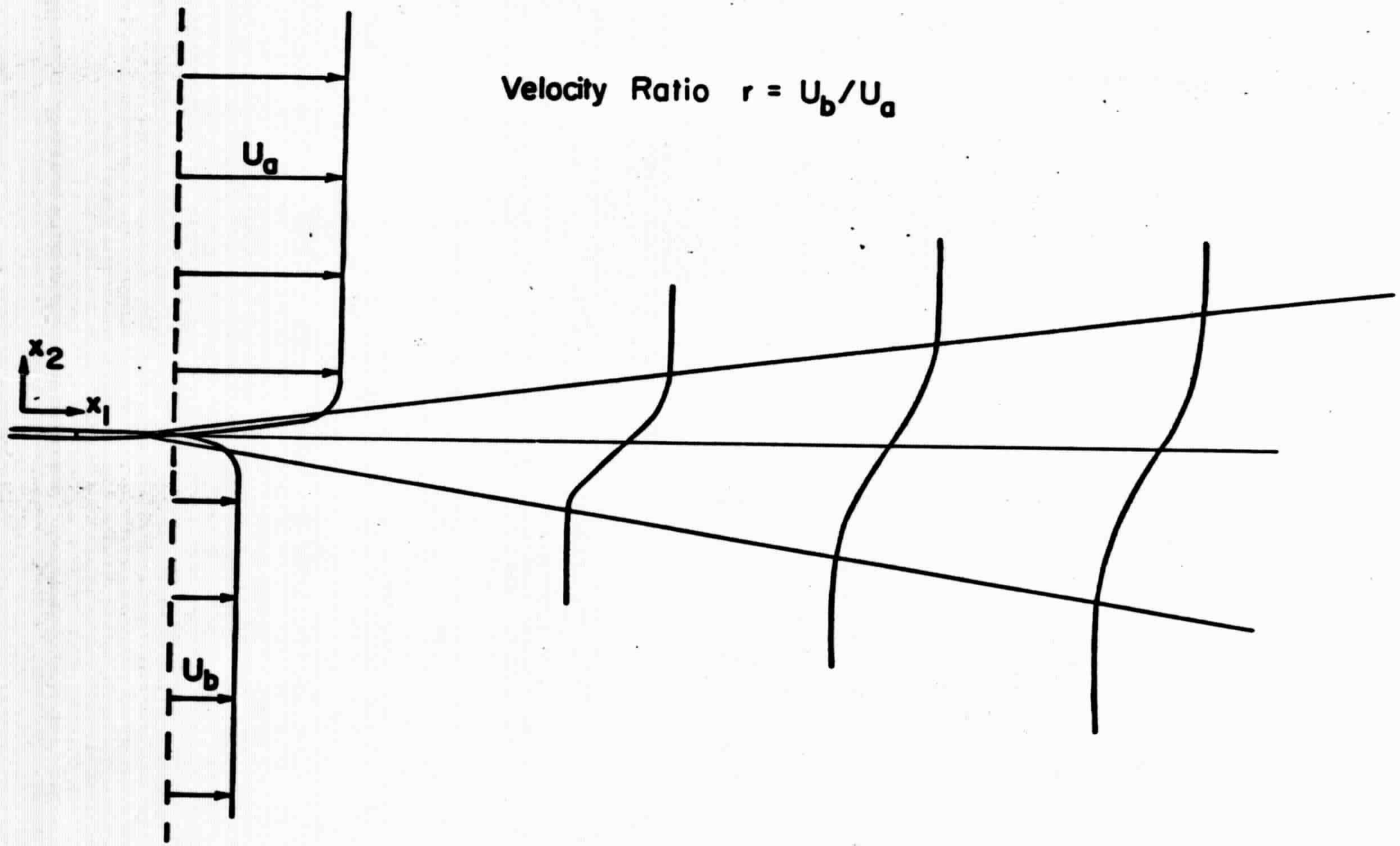

Figure 1 The mixing of two parallel, uniform streams of fluid.

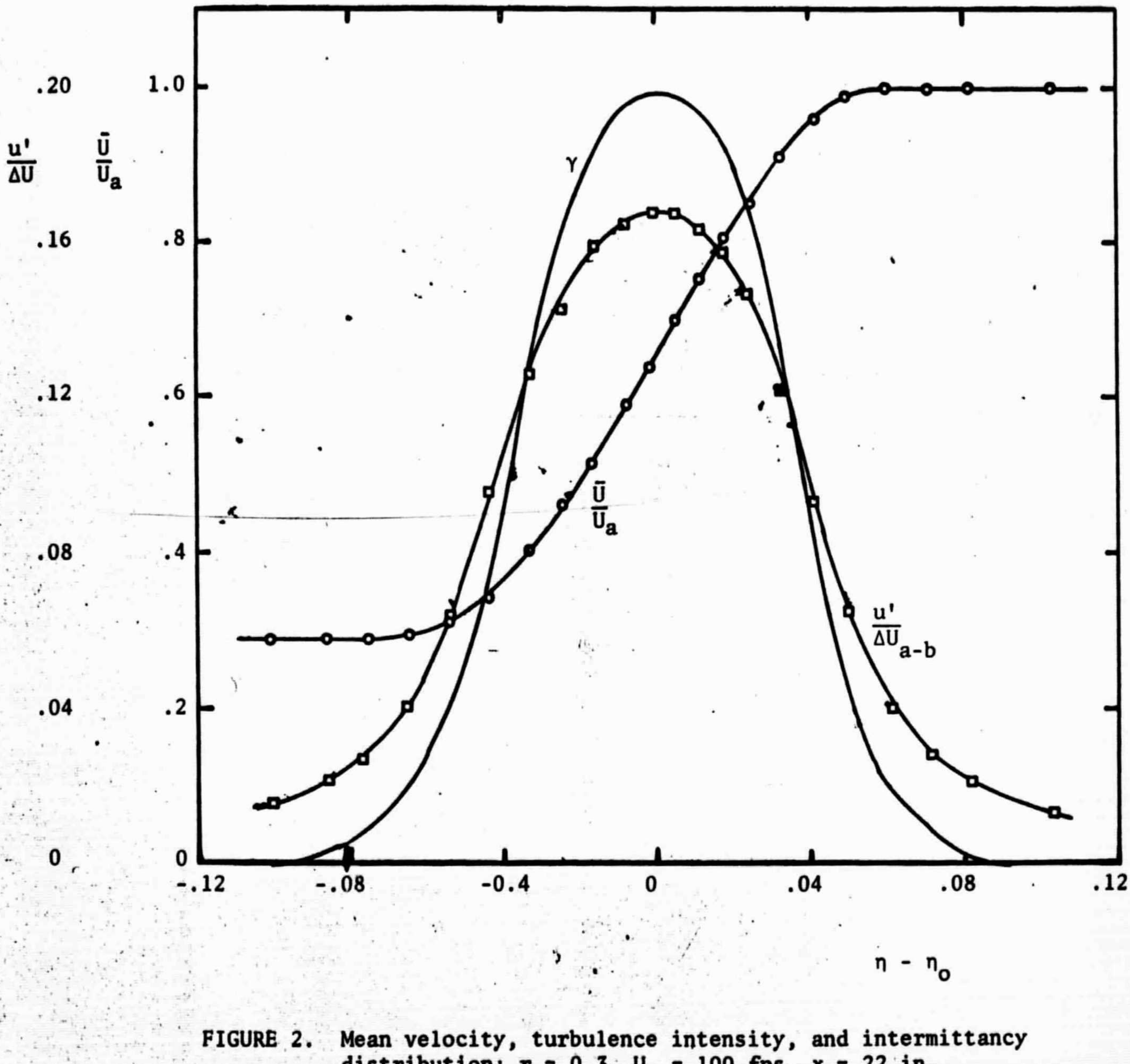

FIGURE 2. Mean velocity, turbulence intensity, and intermittancy distribution; $r = 0.3$, $U_a = 100$ fps, $x = 22$ in.

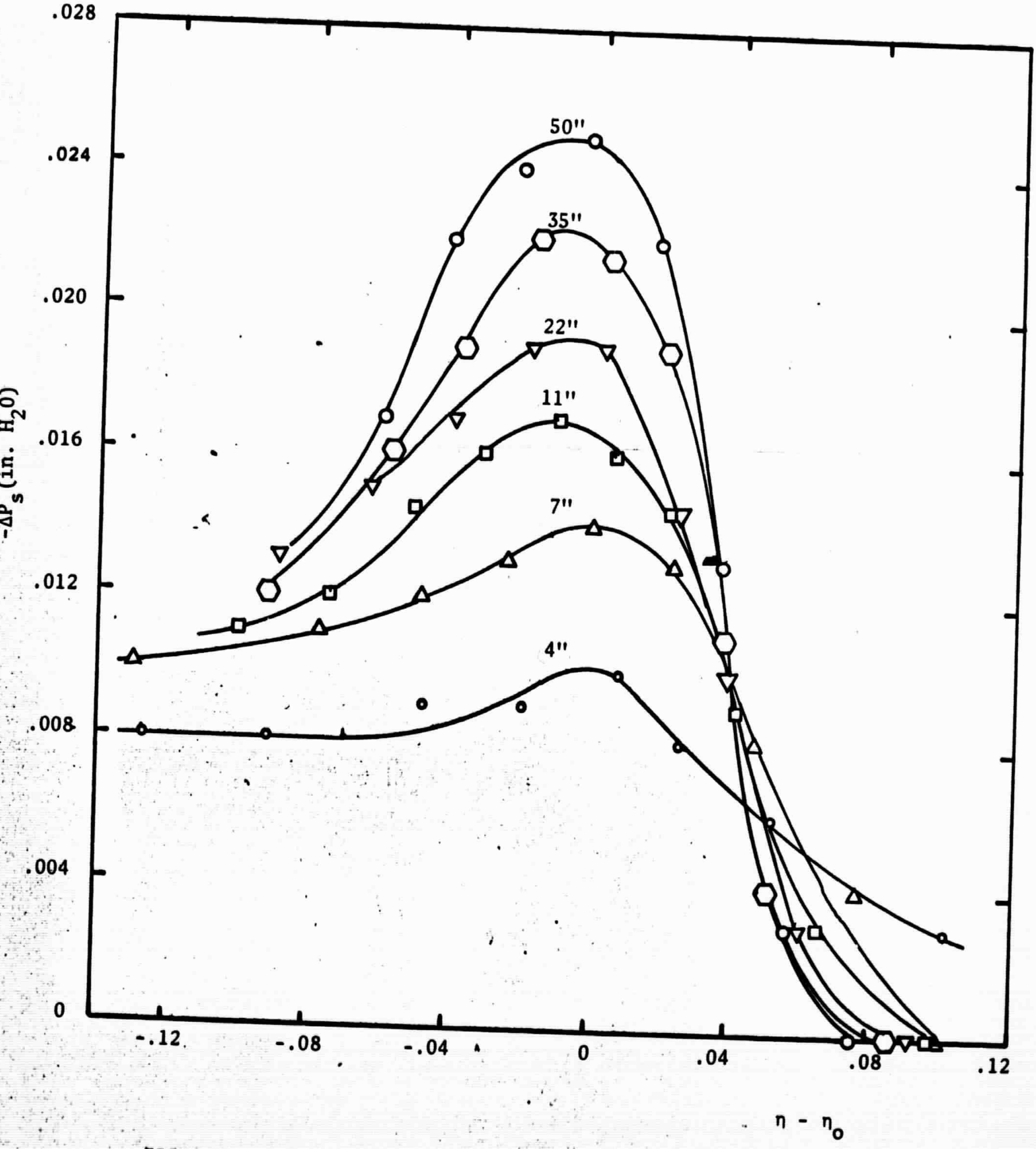

FIGURE 3. Development of mean static pressure distribution; $r = 0.3$, $U_a = 100$ fps.

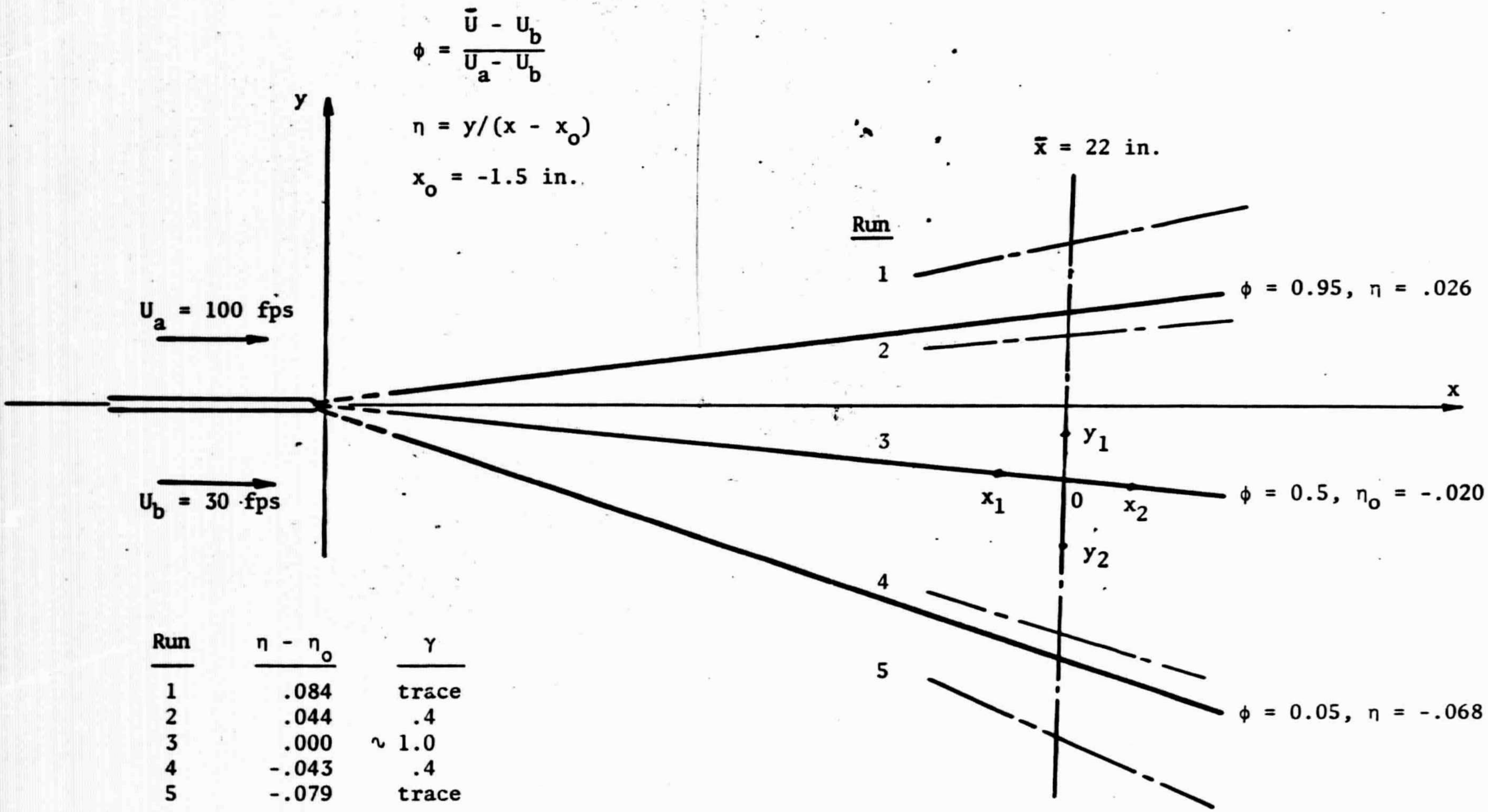

Run	$\eta - \eta_o$	γ
1	.084	trace
2	.044	.4
3	.000	~ 1.0
4	-.043	.4
5	-.079	trace

FIGURE 4. Locations and conditions for correlation measurements in fully-developed two-stream mixing layer.

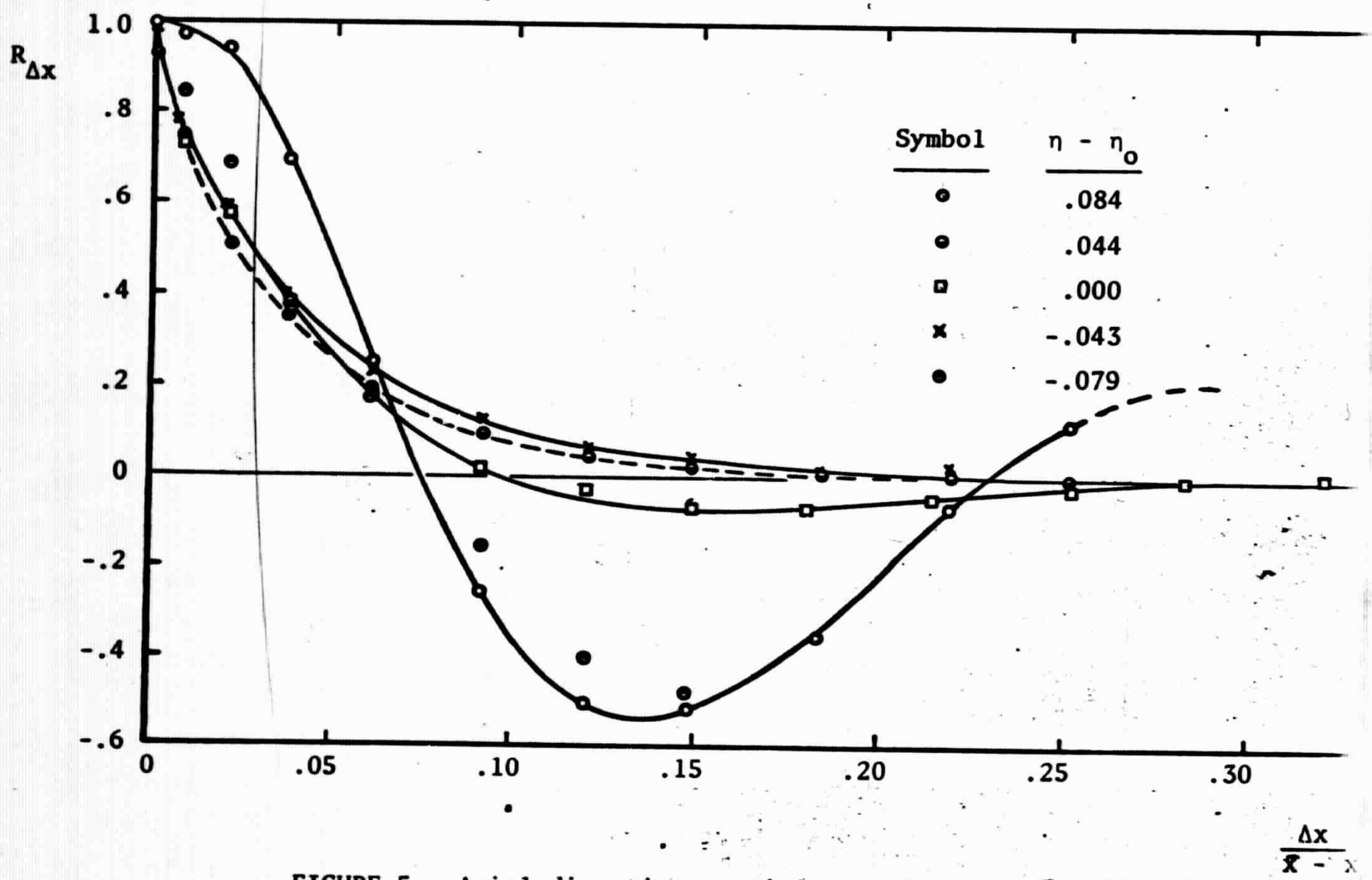

FIGURE 5. Axial direction spatial correlations; $\bar{x}$ = 22 inches.

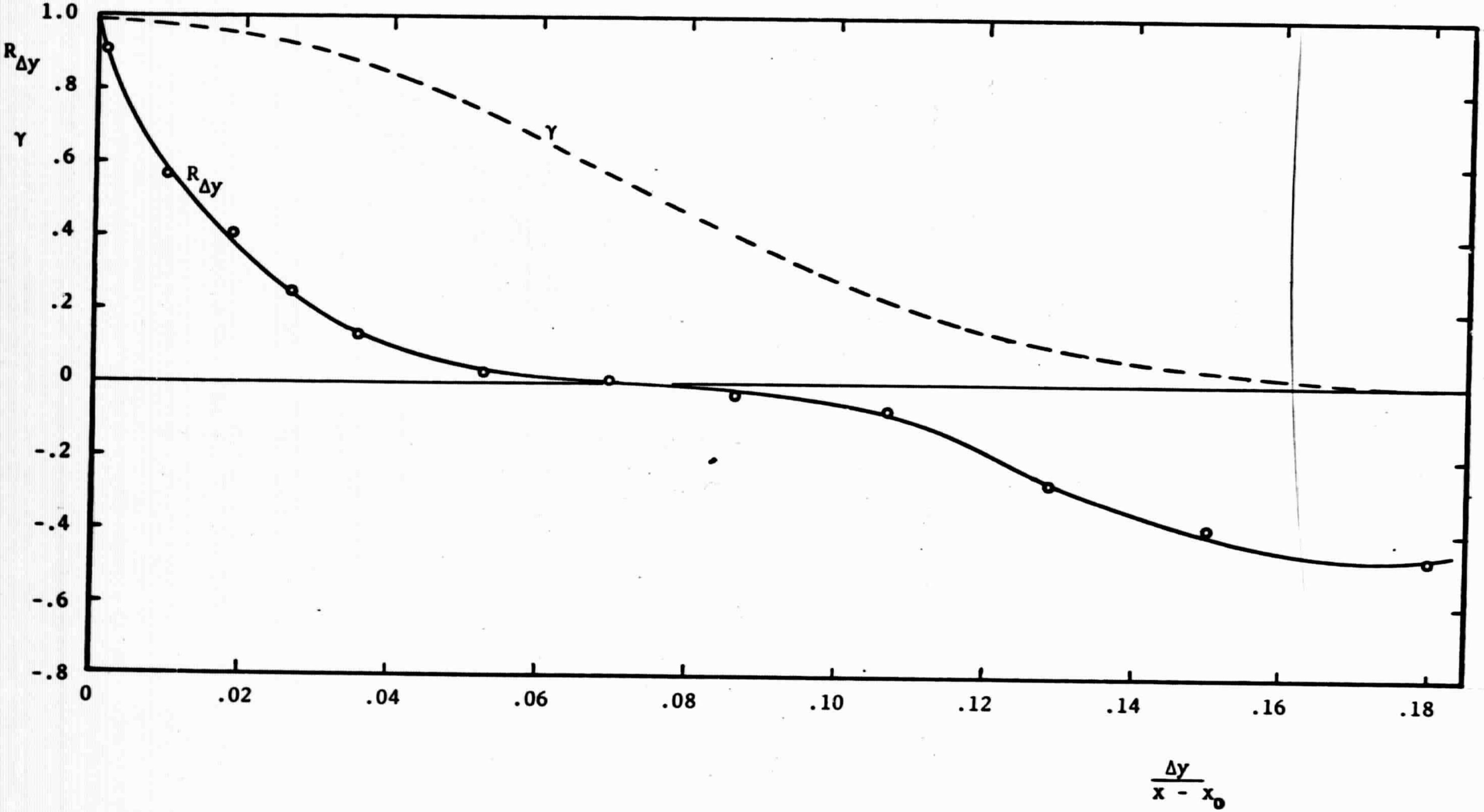

FIGURE 6. Transverse direction spatial correlation centered about $\phi = 0.5$; $x = 22$ in.

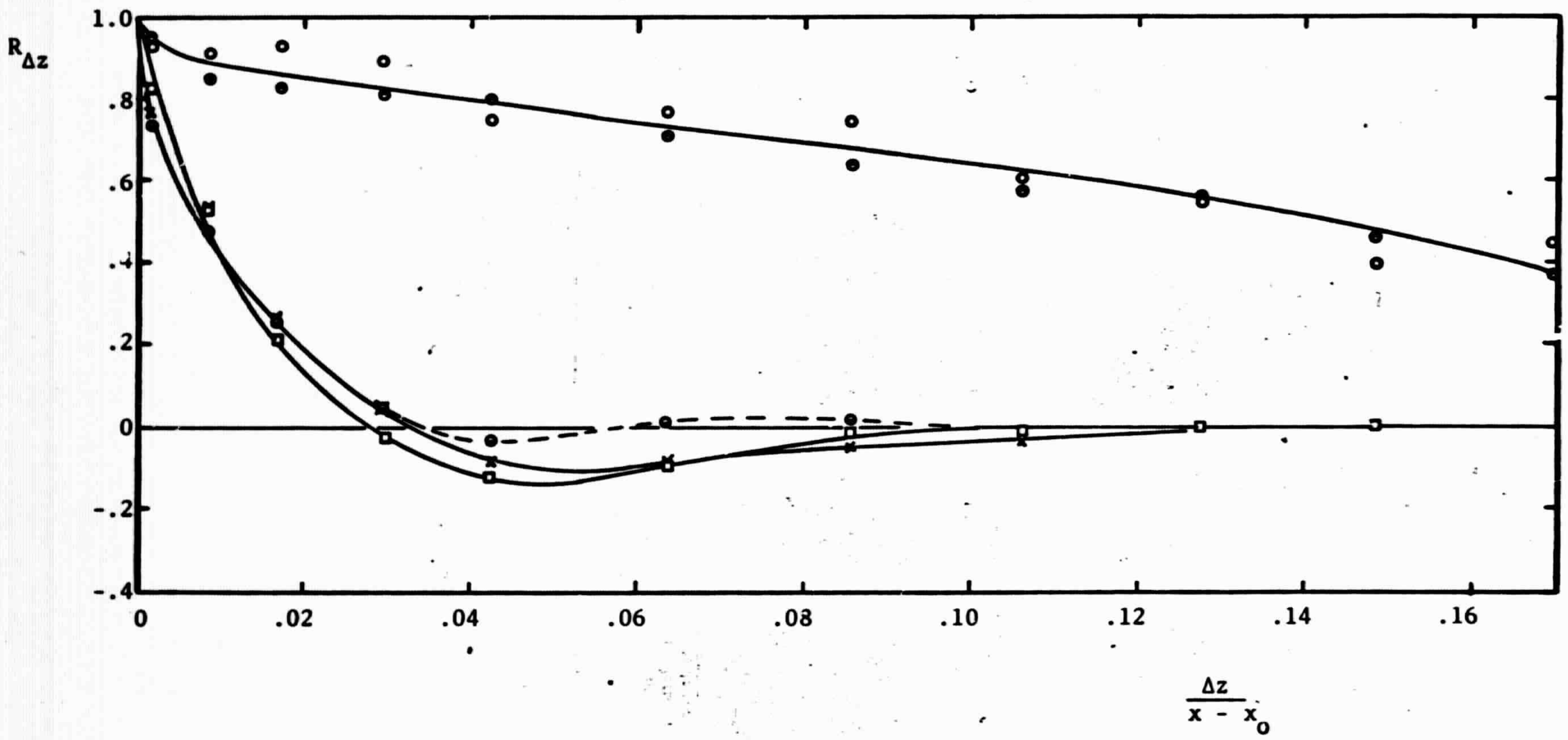

FIGURE 7. Lateral direction spatial correlations; see legend on Fig. 5 x = 22 in.